Nonlinear Dynamics, Psychology, and Life Sciences, Vol. 27, No. 3, pp. 259-289.

The Mathematical Characterization of the Complexity Matching during a Healing Circle Meditation

Naseha Wafa Qammar,[1] ***Minvydas Ragulskis****, Kaunas University of Technology, Kaunas, Lithuania****, Roza Joffe-Luiniene, Alfonsas Vainoras****, The Lithuanian University of Health Sciences, Kaunas, Lithuania,* ***Nachum Plonka, Mike Atkinson, Rollin McCraty, Carla Stanton****, HeartMath Institute, Boulder Creek, CA, and* ***Joe Dispenza****, Encephalon, LLC, Rainier, WA*

Abstract: *The aim of the study is to evaluate the complexity matching between the HRVs of the group of Healers and the Healee during the various stages of the meditation protocol by employing a novel mathematical approach based on the H-rank algorithm. The complexity matching of heart rate variability is assessed before and during a heart-focused meditation in a close non-contact healing exercise. The experiment was conducted on a group of individuals (eight Healers and one Healee) throughout the various phases of the protocol over a ~75-minute period. The HRV signal for the cohort of individuals was recorded using high-resolution HRV recorders with internal clocks for time synchronization. The Hankel transform (H-rank) approach was employed to reconstruct the real-world complex time series in order to measure the algebraic complexity of the heart rate variability and to assess the complexity matching between the reconstructed H-rank of the Healers and Healee during the different phases of the protocol. The integration of the embedding attractor technique was used to aid in the visualization of reconstructed H-rank in state space across the various phases. The findings demonstrate the changes in the degree of reconstructed H-rank (between the Healers and the Healee) during the heart-focused meditation healing phase by employing mathematically anticipated and validated algorithms. It is natural and thought-provoking to contemplate the mechanisms causing the complexity of the reconstructed H-rank to come closer; it can be explicitly stated that the purpose of the study is to communicate a clear idea that the H-rank algorithm is capable of registering subtle changes in the healing process, and that there was no intention of delving deep to uncover the mechanisms involved in the HRV matching. Therefore, the latter might be a distinct goal of future research.*

Key Words: Hankel matrix, meditation, complexity matching, attractors, heart rate variability

[1] Correspondence address: Naseha Wafa Qammar, Department of Mathematical Modelling, Kaunas University of Technology, LT-51368 Kaunas, Lithuania. E-mail: naseha.qammar@ktu.edu

INTRODUCTION

Before we begin describing the introduction section of this study, it is considered imperative to outline the study structure while keeping the research's main objectives and targets in mind. The main objective of this study is to introduce the notion of the H-rank technique as a reliable and efficient mathematical method for identifying complexity matching between the HRVs of the group of individuals known as Healers and the Healee during the meditation exercise. It should also be emphasized that when we mention about the complexity of the HRV, we effectively mean the number of algebraic components required to reconstruct the given HRV time series with a given accuracy (epsilon). With the study's purpose in mind, the following arrangement will be followed in the Introduction section: We will begin our study introduction by first describing the (a) human interactions and synchronization, then (b) meditation, its various styles and psychological impacts, (c) heart rate variability as the measure of the complexity, and lastly (d) Measuring complexity with the H-rank technique.

Human Interactions and Synchronization

Study of synchronization between the human within groups and with the outside world are prominent fields of study in psychology, psychophysiology, clinical and the social and environmental sciences. There can be various setups when persons are performing coordinated activities (Guastello & Peressini, 2017), for example watching an orientation video together, an individual decision task, and a group decision task (Guastello, Mirabito, & Peressini, 2020), or the persons may be connected due to the physiological activity (Palumbo et al., 2017), or the coordinated activity exists between or among the individuals for a shared objective (Kazi et al., 2021); in all scenarios, the synchronization appears to take place in time. Observations from everyday life show that widespread coherent activities among people are associated with successful interpersonal relationships (Zhang, Meng, Hou, Pan, & Hu, 2018). During social interaction, people tend to contemporize with individuals with whom they desire to build favorable relationships (Miles, Lumsden, Richardson, & Neil-Macrae, 2011) and the coherent flow in social interactions largely depends on the unconscious harmony between people (Cohen, Janicki-Deverts, Turner, & Doyle, 2015; McCraty, 2004, 2017; Murphy, Janicki-Deverts, & Cohen, 2018). When we are engaged in conversation, we unconsciously begin to coordinate our movements, postures, speaking rates and length of pauses (Cleeland et al., 1994). A growing body of literature has shown that important aspects of people's physiology also can become same (Cohen et al., 2015).

The coordination of the rhythmic activity among separate individuals requires some type of a signal (chemical, light, tactile, electromagnetic, or sound) to convey information between them. For example, the matching of physical activities through visual cues has been shown to increase compassion and altruistic behavior (Vacharkulksemsuk & Fredrickson, 2012; Valdesolo & DeSteno, 2011), and pro-social behaviors (Steinhoff et al., 2004). Examining

synchronized brain activity in groups is of interest in social neuroscience, however, the ability to conduct studies in real-world social contexts or in groups is methodologically challenging, due to the lack of suitable recording set-ups and appropriate tools for multi-participant analysis. Multiple studies have demonstrated brain-to-brain synchronization in pairs of participants suggesting that the perceptual systems of one person's brain can be coupled or linked to another person's brain (Fusaroli & Tylén, 2012) and has been suggested as a mechanism for extended consciousness and group consciousness, potentially explaining the known association of contemporation with the feeling of being together with someone else (Valencia & Froese, 2020). For example, in functional magnetic resonance imaging (fMRI), studies have demonstrated synchronization between listener and speakers' brains which exhibit coupled temporal response patterns during communication and more extensive neural coupling, which was associated with more successful communications (Stephens, Silbert, & Hasson, 2010). The increased interest in fMRI (Bilek et al., 2015; Koike et al., 2016; Schippers, Roebroeck, Renken, Nanetti, & Keysers, 2010; Stephens et al., 2010; Tanabe et al., 2012) and electroencephalography (EEG) in physiological synchronization research (Astolfi et al., 2010; De Vico Fallani et al., 2010; Kawasaki, Yamada, Ushiku, Miyauchi, & Yamaguchi, 2013) has revealed that verbal and nonverbal communication promotes interpersonal links between brain activity (Timofejeva et al., 2017).

In a study examining patient-clinician interactions during simultaneous fMRI recordings, clinicians interacted with the patient via live video, during the treatment of evoked pain in patients with chronic pain (Ellingsen et al., 2020). The results showed that patient analgesia was mediated by patient-clinician nonverbal behavioral mirroring and extensive dynamic brain-to-brain synchronization in circuitry associated with social mirroring, but only in dyads where pre-established clinical rapport was established. There is numerous evidence showing that close contact with another person significantly reduces viral illness, strengthens immunity, and for those who are already ill, having contact with someone improves the course of the disease and relieves the occurrence of severe symptoms (Cohen et al., 2015). Close contact has also been shown to have a positive effect on the dynamics of interpersonal conflicts (Murphy et al., 2018), the stabilization of blood pressure and heart activity (Light, Grewen & Amico, 2005). Identification of clusters in a group of people is an important aspect in this context, and psychologists have been using various questionnaires to identify sub-groups of people based on their psychological traits. This has been done with various purposes, such as anticipating the success of intimate relationships (Lucchi, Basili, & Sacco, 2020), effective leadership and team dynamics (Delice, Rousseau, & Feitosa, 2019) etc. However, when observing human behaviors and interactions, more complex dynamics than the compatibility of psychological traits become apparent. Relevant to this study, a study of shared intentionality where individuals had a shared goal and needed to coordinate their efforts, functional near-infrared spectroscopy was used to demonstrate a significant increase in interpersonal neural synchronization

between the pre-frontal cortex of participant pairs engaged in a mutually held goal (Fishburn et al., 2018). In contrast, when participants were engaged in identical, but individual-focused goals significant interpersonal neural synchronization were absent.

In a nutshell, synchronization phenomena exist in different complex dynamical systems. For example, clocks, chirping crickets (Strogatz, 2003), cardiac pacemakers, firing neurons, and applauding audiences all tend to operate in tandem. These phenomena are widespread and may be characterized with a paradigm based on current nonlinear dynamics (Pikovsky, Rosenblum, & Kurths, 2001; Sulis, 2016).

In the next section, we will discuss meditation in general, its various types, and the psychological interactions that occurs as a result of meditation.

Meditation, Its Various Styles and Psychological Impacts

The health effects of various types of meditation are another important aspect to consider when discussing the complex dynamics of human health and healing. Meditation has been practiced over millennia by diverse groups of people in many different traditions, has widely spread into Western society and is quite often used as a therapeutic approach to facilitate healing (Behan, 2020). In general, meditation could be described as a process of concentrating on your inner self and expanding consciousness or awareness beyond one's normal day-to-day experience (Sharma, 2015), in many cases involving a specific intention to connect with another person to facilitate healing (Lindhard, Hermann, & Edwards, 2021). According to one study, mindfulness meditation has significant impacts on brain and immunological functions (Davidson et al., 2003). Meditation has been shown to increase the activity in the prefrontal cortex, the cingulate cortex and the hippocampus, and to decrease activity in the amygdala, resulting in better emotion regulation (Gotink, Meijboom, Vernooij, Smits, & Hunink, 2016). Meditation has also been shown to reduce age-related brain degeneration (Khalsa, 2015; Luders, 2014; Newberg et al., 2014) and improve prospective and spatial memories (Lardone et al., 2018). In addition, meditation has been positively associated with reduction of anxiety, depression, rumination and overall improvement in mood control (Afonso, Kraft, Aratanha, & Kozasa, 2020; Zhang, Wang, Wang, Liu, & Huang, 2019) which is related to physiological indicators such as HRV, blood pressure and others.

There are many styles of meditation that suggest different ways to redirect one's focus and attention, although some share similar approaches, they can have different theoretical orientations. Many approaches to meditation focus on attempting to still one's mind and thoughts while others such as HeartMath's Heart Lock-In and there are some Buddhist meditations which focus specifically on cultivating feelings of appreciation, unconditional loving-kindness, and compassion. In a study of Zen monks, who focus on generating positive feelings, it was found that the more advanced monks tended to have coherent heart rhythms, while the novices did not (Lehrer et al., 1999). In a number of studies that have used the Heart Lock-In technique, it has been shown that it results in a significant

increase in heart rhythm coherence, which is associated with a wide range of mental, emotional and physiological benefits (Lehrer, Sasaki, & Saito, 1999; McCraty, 2017; McCraty, Atkinson, Tiller, Rein, & Watkins, 1995; McCraty, Atkinson, Tomasino, & Bradley, 2009).

The new tools that have been developed for the study of non-linear, complex dynamic systems offer a promising area for new systematic research in the study of HRV complexity and how it may be facilitated by meditation practices that increase physiological coherence (Timofejeva et al., 2021). In the next section we will elaborate about the HRV as an efficient measure of analyzing the complexity of the signal.

Heart Rate Variability as a Measure of Complexity

An approach for evaluating physiological communication between individuals and between people and environmental influences, such as the resonant frequencies in the Earth's magnetic fields is the heart rate variability (HRV). HRV is the measurement of the change in the time intervals between successive pairs of heartbeats, is an emergent property of interdependent regulatory systems which operate across different time scales to adapt to environmental and psychological challenges (McCraty & Shaffer, 2015). HRV provides a widely validated means to evaluate changes in the autonomic nervous system (ANS) dynamics in real-time, in ambulatory contexts, with no technical limit on the number of participants that can be recorded simultaneously with synchronized timing. It, therefore, provides an ideal assessment for studying the real-time, complex dynamics of groups and psychological activity.

All analyses of HRV are conducted on the R–R (R-wave of the ECG) intervals, which can be done over various time frames. These intervals may then be examined by employing time or frequency domain analysis (Martinmäki & Rusko, 2008), nonlinear analysis (de Godoy, 2016), and chaotic analysis (Naghsh, Ataei, Yazdchi, & Hashemi, 2020). Because of the nonlinear nature of the HRV signal, nonlinear techniques may be employed to analyze HRV signals efficiently (Voss, Schulz, Schroeder, Baumert, & Caminal, 2009). Nonlinear techniques can describe the hidden dynamics of the ANS and cardiovascular system (Steven, 2010).

The human body is a complex system (Clermont & Angus, 2001; Ladyman, Lambert, & Weisner, 2013) in which many different systems within the body must work together in coherence to maintain life's functions. A complex and constantly variable heart rate (HR) indicates the presence of robust regulatory mechanisms capable of successfully adjusting to environmental and psychological challenges and stressors (Lombardi, Malliani, Pagani, & Cerutti, 1996; Obrist, 2012; Selye, 1956; Vila et al., 2007) while decreased age-adjusted HRV is associated with poor self-regulatory capacity, cardiovascular and vascular diseases (Obrist, 2012) and mental and cognitive disorders (Stein et al., 2000; Taylor, 2010; Tulen et al., 1996). Due to the fact that the interdependent underlying physiological sources of HRV work across various time scales, the frequencies found in the heart's rhythm are distributed in different frequency

bands. Because it can distinguish sympathetic from parasympathetic control of the sinoatrial node, the mathematical transformation of HRV is frequently utilized as a noninvasive test of integrated neurocardiac function (Ziemssen & Siepmann, 2019). Due to the convenience and low cost of HRV data collection, as well as its clinical health significance and strong correlations with psychophysiological variables, the use of HRV in research has flourished over the last several decades (Pham, Lau, Chen, & Makowski, 2021), including physiological synchronization studies (McCraty, 2004, 2017; McCraty et al., 2017; Pérez et al., 2021; Timofejeva et al., 2021; Yoon et al., 2019).

As stated above, for the physiological activity of separate individuals to map, a signal of some type is needed to convey information between the individuals. The role of visual, tactile, and auditory signals as the mediating signal for the physiological communication between participants has been explored.

Measuring Complexity with the H-rank Technique

The dynamical principles that govern human physiology are far from linear, necessitating an examination of nonlinearity that exists in the dynamical systems. For example, physiological data such as EEG, ECG, and fMRI, gene expression data, etc., can be characterized as nonlinear time series. In order to describe the underlying dynamical system of a given nonlinear time series, a few characteristic values are often taken from a wide sample of the data sets. As a result, the compressed information represented by these characteristic numbers must highlight certain system properties (Zou, Donner, Marwan, Donges, & Kurths, 2019). The fast evolution of dynamical systems theory, sometimes known as" chaos theory," which examines system dynamics using a set of nonlinear difference equations, gives way to the collection of nonlinear time series analytical concepts and approaches. Many mathematical techniques have been used to solve the nonlinear system. Nonlinear stochastic approaches, data-based mechanistic models, artificial neural networks, support vector machines, wavelets, evolutionary computing, fuzzy logic, entropy-based techniques, and chaos theory are just a few of the methodologies (Sivakumar, 2017).

For systems identification, the Hankel matrix, named after Hermann Hankel, is often implemented. For instance, in a method for clocking the convergence of iterative chaotic maps, the Hankel rank concept is used (Ragulskis & Navickas, 2011). The H-rank approach is presented by (Ragulskis, Navickas, Palivonaite, & Landauskas, 2012) to decompose the solution into algebraic primitives. The notion of the H-rank is used by (Ragulskis, Lukoseviciute, Navickas, & Palivonaite, 2011) to find a base fragment of the time series. As previously stated, the adaptability of the H-rank approach lies in the fact that it aids not only in the study of complex time series such as HRV, but also in determining the number of algebraic components required to reconstruct the given time series with the given accuracy (the threshold parameter epsilon) (Ragulskis et al., 2012).

Before we single out the H-rank algorithm to establish a precedent for identifying the complex dynamics of the HRV. It is worth mentioning to state the

fact that the comparative analysis of other algorithms with H-rank is beyond the scope of this paper. However, we would want to highlight the degree of complexity associated in dealing with HRV signal and the adaptability of the H-rank algorithm to deal with complex time series contaminated by noise yields promising results (Ziaukas, Alabdulgader, Vainoras, Navickas, & Ragulskis, 2017). Of course, implementing other mathematical algorithms and their comparison with the H-rank technique can be said to serve as the objective of future research.

With the utility and adaptability of the H-rank approach for analyzing diverse nonlinear systems (Landauskas, Navickas, Vainoras, & Ragulskis, 2017; Ragulskis et al., 2012), we do implement it on HRV data. The primary goal of this study is to analyze the complexity matching between the HRVs of the group of Healers and the Healee during the various stages of the meditation protocol. Our method is distinctive in that we use the Hankel matrix-based approach to examine the algebraic complexity matching of the HRV data for a cohort of individuals (Healers and the Healee). When the HRV of the Healers and Healee exhibit similar H-rank, this suggests that there is relationship in the form of complexity matching. The concept of complexity matching used in this paper is closely related to synchrony which is also discussed in the following studies on dyadic interaction where researchers examined the processes of synchronization, entrainment, alignment, and convergence and proposed a coordination term known as complexity matching (Abney, Dale Paxton, & Kello, 2014; Fine, Likens, Amazeen, & Amazeen, 2015).

METHODS

Participants

The study population consisted of nine female volunteer meditators attending a 7-day meditation retreat in the USA, led by Dr. Joe Dispenza in September 2019. During the retreat over 1000 attendees were guided through a series of lectures by Dr. Dispenza regarding the mind-body connection and participated in ~35 hours of meditation varying in intent and posture (including sitting, standing, lying, walking, and healing focused meditations). It should be noted that the meditation was guided, but no control mechanisms were involved. When we mention about control mechanisms, we are addressing the fact that there are no intentions to influence the healers.

Prior to the retreat, all attendees were invited via email to volunteer in HRV research during the event. Over 600 attendees (mostly female) volunteered to take part and completed an online HIPAA compliant application form capturing their name, gender, date of birth, pre-existing health conditions, current meditation, and consent.

After excluding applicants who did not fit the inclusion criteria (i.e., those on heart rhythm altering medications which could invalidate HRV data accuracy), 92 healthy applicants were selected at random and 8 participants with pre-existing (non-cardiac) health conditions were selected to be Healees. The 100

selected participants were then divided into groups of 20, and each day (for 5 consecutive days of the retreat) a new group of 20 participants were fitted with the HRV recorders.

All participants underwent 24-hour ambulatory HRV recordings using high-resolution HRV recorders (Bodyguard2, first beat Technologies Ltd., Jyväskylä, Finland) which were attached by the site coordinator. Ambu Blue Sensor L microporous disposable electrodes were located in a modified V5 position. The inter-beat-interval (IBI) was calculated by the HRV recorder from the electrocardiogram with a sample rate of 1000 Hz. The RR intervals were stored in the HRV recorders' memory. The HRV data were then downloaded to a workstation and edited for artifacts from moment and ectopy using DADiSP 6.7. IBIs less or greater than 30% of the mean of the previous four intervals were removed from the analysis record. Following the automated editing process, all recordings were reviewed manually by an experienced technician and, where needed, corrected. All the HRV recordings were segmented into consecutive 5-min segments. Any 5-min segment with more than 10% of the IBIs either removed or missing were excluded from the analysis. The local time stamps in the HRV recordings were used for time synchronization between participants.

The HRV data analyzed here is from 9 of the participants during a close non-contact healing exercise that took place over ~75 minutes on September 21st, 2019. All 9 participants were female, aged between 33-67 (mean age of 48 years) and all healthy subjects other than the 1 Healee (56 years old) who was selected due to their pre-existing (non-cardiac) medical condition (-lung fibrosis post pneumonia). All Healers had limited interaction with their Healee prior to the healing protocol and were unaware of their Healee's medical diagnosis.

Ethics Statement

The research met all applicable standards for the ethics of experimentation in accordance with the Declaration of Helsinki as reflected in prior approval by the Regional Biomedical Research Ethics Committee of the Lithuanian University of Health Sciences (ID No. BE-2-4, 15 March 2016). The permit to perform biomedical investigation was granted by the (copies of documents are enclosed as Supplementary Materials). Participants provided written informed consent prior to the experiment.

Experiment

The healing protocol lasted for ~75 minutes and consisted of 9 phases. After the Healers gathered (Phase 1), the meditation phase began with Healers standing up and closing their eyes for fifteen minutes (Phase 2). All Healers then opened their eyes and began walking around the conference room for eleven minutes (Phase 3). After a brief period of returning to the standing meditation phase (Phase 4, eyes closed), all Healers opened their eyes and formed circles of 8 Healers (Phase 5). The Healees then entered the room and took their positions in the healing circle (Phase 6). The Healers then sat down around their Healee and

began a heart-centered meditation (Phase 7). All Healees then rubbed their own hands together and extended their hands towards the Healee (Phase 8). This is the

Table 1. Timing of the Nine Phases of the Synchronization Shifts.

	Local Time		*Seconds*		
Phase	*Start*	*End*	*Start*	*End*	*Description*
1	17:00	17:06	0	360	Healers assemble: All Healers gather and stand waiting outside the conference (healing) room prior to the healing protocol.
2	17:06	17:21	360	1260	Standing meditation part 1: Healers participate in the standing section of the guided healing meditation (eyes closed).
3	17:21	17:32	1260	1920	Walking meditation: Healers open their eyes and walk in a large circle around the room to the guided healing meditation (eyes open).
4	17:32	17:35	1920	2100	Standing meditation part 2: Healers stop, close their eyes and stay standing during final guided Healers meditation.
5	17:36	17:39	2160	2340	Healing-circle formation: Healers open their eyes and form healing-circles (in groups of 8).
6	17:39	17:51	2340	3060	Healees enter healing-circle: Healees enter the healing room, lie down in the center of the healing circles, and close their eyes. (Healers remain standing with eyes closed throughout).
7	17:51	18:01	3060	3660	Healers and Healees connect: Healers open their eyes, sit down, and look at their Healee and other Healer's briefly, then close their eyes to begin a guided heart-focused meditation.

(Continued)

Table 1. *Continued*.

	Local Time		*Seconds*		
Phase	*Start*	*End*	*Start*	*End*	*Description*
8	18:01	18:07	3660	4020	Healers intend to influence the Healee: All Healers rub their own palms together, before pointing their hands in the direction of the Healee and meditate on creating a coherent energetic field around Healee.
9	18:07	18:15	4020	4500	Healers conclude the Healing Meditation: All Healers place their own hands over their hearts and are guided to meditate on directing their heart energy inward, which concludes the healing meditation protocol.

moment when the Healers intend to direct their elevated individual energy to the Healee, and then synchronize this with the collective energy of all Healers, thus creating a coherent energetic field around the Healee. Finally, the Healers laid their hands over their own hearts, indicating the conclusion of the healing meditation protocol (Phase 9). See Table 1.

The next section presents and defines the computational techniques used to interpret the recorded HRV for both the Healers and the Healee, followed by an explanation of the phase plane representation of the healing process throughout the experiment.

H-rank Algorithm Adaptability for Synthetic Data

This section will provide a summary of the Hankel matrix and the mathematical form of the Hankel transform. Later, we shall describe the adaptability of the H-rank approach by analyzing the chaotic time series as an example, which we will refer to as synthetic data. Finally, the applicability of the H-rank is demonstrated using the complex time series (RR-cardiac interval) exploited in our research.

A Hankel matrix:

$$\mathrm{x}\ \mathrm{A_n} = \begin{bmatrix} c_0 & c_1 & \cdots & c_{n-1} \\ c_1 & c_2 & \cdots & c_n \\ \vdots & \vdots & \ddots & \vdots \\ c_{n-1} & c_n & \cdots & c_{2n-2} \end{bmatrix}$$

is a matrix (a_{ij}) in which for every r the entries on the diagonal $i + j = r$ are the same, i.e., $a_{i,r-j} = c_r$ for some c_r. If we consider a scalar time series of real numbers $\{x_j\}_{j=1}^{+\infty}$. The Hankel transform maps this series into a sequence $\{h_j\}_{j=1}^{+\infty}$,

where h_j = det (H_j) and H_j is a j-order catalectican Hankel matrix:

$$H_j = \begin{bmatrix} x_1 & x_2 & \cdots & x_j \\ x_2 & x_3 & \cdots & x_{j+1} \\ \vdots & \vdots & \ddots & \vdots \\ x_j & x_{j+1} & \cdots & x_{2j-1} \end{bmatrix}$$ (Tamm, 2001).

The H-rank algorithm was demonstrated in (Landauskas et al., 2017; Palivonaite & Ragulskis, 2014; Ragulskis et al., 2011) and has been widely employed to determine not just the order of a linear recurrence sequence, but also to evaluate algebraic complexity of complex time series. We shall recall the primary goal of this research, which is to identify the complexity matching between the Healers and the Healee throughout the meditation exercise by registering the RR cardiac interval. The analysis of complex time series (such as RR cardiac intervals) demands the utilization of credible computation techniques in order to determine the number of algebraic components required to reconstruct the original time series. As a result, in order to fully comprehend the functioning of the H-rank algorithm for the RR cardiac interval, we will first thoroughly assess the H-rank method's applicability on synthetic data. The synthetic data we intend to examine in our study is the Master Slave coupling logistic map equations. The intent of employing the synthetic chaotic time series as an example, is to demonstrate how efficient the H-rank technique is in determining the algebraic components required to reconstruct the original complex time series and then visualize the synchronization between the two systems.

Consider the model of the master slave coupled logistic map (MSC; Brown, Rulkov, & Tracey, 1994); we refer to this example as synthetic data. As the model's name implies, the primary system is "master," and the secondary system is "slave;" the slave only follows the master. The MSC model is analyzed using the H-rank algorithm in order to demonstrate its capability to detect the synchronization between the two systems. It should be emphasized that the term "synchronization" refers to the "complexity matching" as mentioned earlier. Many types of chaos synchronization can be observed in coupled chaotic systems for instance amplitude envelope synchronization (González-Miranda, 2002), lag synchronization (Sun, Wang, Wang, & Wu, 2015) and others etc., (Ahmadlou & Adeli, 2012; Hoon, Mohd Radzi, Mohd Zainuri, & Zawawi, 2019; Wang, Wen, Yu, Yu, & Huang, 2018). We will examine the master slave coupled synchronization by analyzing the model with H-rank technique.

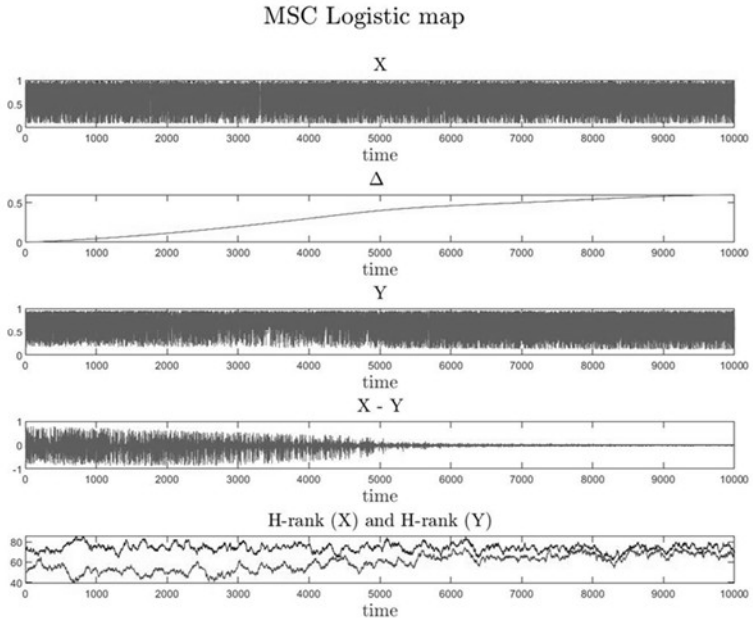

Fig. 1. The complexity matching revealed by the H-rank algorithm can identify the synchronization between the "master" and the "slave" in MSC logistic maps. The first panel of the figure shows the original time series x(t)-which is the master. The second panel of the figure contains the values of delta. The following figure shows the slave time series y(t). The second last figure panel exhibits the difference between time series X and Y. The last figure of the panel shows the H-rank computed for the master and the slave.

The equations of the MSC model read:

$$x_{k+1} = r_x\, x_k\, (1 - x_k) \tag{1}$$

Equation 1 does represent the paradigmatic logistic map. The variation range of the discrete variable x_k is limited between 0 and 1 when the initial condition x_0 is between 0 and 1, and the parameter r_x is in the range [0, 4]. We choose $x_0 = 0.1$ and $r_x = 3.9$ what guarantees that the dynamics of the "master" is chaotic.

$$\mathrm{y_{k+1}} = \mathrm{r_y\, y_k\, (1 - y_k)} \tag{2}$$

Equation 2 does represent the "slave" in the model of MSC logistic map. The value of parameter r_y is set to 3.89.

$$q_k = \Delta\ x_k + y_k\, (1 - \Delta) \tag{3}$$

The third equation defines the coupling between the "master" and the "slave"; the coupling parameter Δ determines the coupling strength. Equations 1 and 2 are completely uncoupled when Δ = 0 (the "slave" is completely free from any impact

from the "master"). Analogously, the "master" and the "slave" get fully coupled when $\Delta = 1$.

In Fig. 1, the first panel of the figure shows the time series $x(t)$ plotted for the first system (the "master"). The second panel of the figure depicts the continuous variation of the coupling parameter Δ. The third panel shows the time series $y(t)$ which refers to the "slave". The fourth panel exhibits the difference between time series $x(t)$and $y(t)$. The last panel depicts the H-ranks computed for both systems, which are plotted on the same graph to visualize the complexity matching during the synchronization of the two systems.

Looking at the graph, it appears that the second system (slave) is acting independently initially. However, as Δ progressively increases, the H-ranks of the two systems appear to synchronize; in other words, the "slave" begins to listen to the "master". The blue graph depicts the H-rank of the first system (the "master"), whereas the red graph depicts the H-rank of the "slave". One can observe that the H-ranks of the two systems are considerably different when Δ is small, and that the evolution of $x(t)$ is far more complicated than the evolution of $y(t)$ due to the difference between parameters of the two logistics maps. However, once the two-time series are in sync, the H-rank of the two systems becomes almost identical, rather than fully identical, because we do not bring Δ to 1. In our case, we did increase Δ only to 0.6. This indeed is a good example to demonstrate the complexity matching between the two systems, which is identified by the means of the H-rank algorithm. In the next section we will describe in detail the adaptability of the H-rank algorithm for the complex time series (RR cardiac interval).

Algebraic Complexity of Time Series Defined by H-rank

The heart rate variability (cardiac RR intervals) of the eight Healers and one Healee was recorded as a time series $\{x_j\}_{j=1}^{+\infty}$. In Fig. 2, the vertical black lines indicate the nine phases of the protocol during the experiment. The blue traces are the HRV of the eight Healers and the red trace is the HRV of the Healee. We apply the H-rank technique to the HRV data to examine the algebraic complexity of the time series using the algorithms illustrates in the previous section. When the Hankel matrix is produced, each row of the Hankel matrix is displaced by one element, and the overlapping between the phases is maximized. The SVD routine is used to produce the standard singular values of the time series. The range of the H-rank matrices in this study is, 150-by-150, which corresponds to 300 data observation points. The lowest and maximum ranges of the matrix are 0 and 150, respectively.

Afterwards, the moving average was also applied to smooth the results of the examined scalar time series data. Many research studies (Hansun, 2013; Hunter, 1986) make use of the moving average approach. The time series data is processed using a three-point simple moving average approach. Each point in the time series data is equally weighted. The algebraic complexity of the time series

data is defined by H-ranks reflecting the mathematical model's backwards memory horizon, which is used to estimate time series data to a given accuracy. It is based on the SVD (singular value decomposition) and the Hankel matrix pseudospectrum (Palivonaite & Ragulskis, 2014).

The following section describes reconstruction of the attractors for the reconstructed H-rank for Healers and Healee during the nine phases of the experiment.

Reconstruction of the Embedded Attractor

This section discusses the implications of the embedding attractor method to visualize the process's state space representation during the different stages of the protocol. The ordered set of embedded points is defined as an attractor, and the 2D plane is known as the state space. One of the characteristics that characterize the dynamics of the time series is the area occupied by the embedded attractor. However, the area of the attractor is determined by the time lag τ utilized for state space reconstruction. We used a simple criterion for determining the area of the embedded attractor, which was based on a direct assessment of the geometric area occupied by the set of points of the trajectory matrix in state space. We consider a finite range of time lag values $\tau = 1 \ldots \tau_{max}$. The maximal value of time lag τ is set to 100. The embedded attractor is reconstructed for the 2-dimensional phase space to visualize the HRV synchronization throughout the experiment. It's worth noting that a scalar time series' Hankel rank is conceptually distinct from the system's state-space realization. The Hankel rank accurately depicts the algebraic relationships between sequence elements without attempting to recreate the analytical model of an underlying dynamical system (Ragulskis et al., 2011). As a result, we reconstruct the embedded attractors from H-rank and their SVD analysis data. For a conventional sine wave, the best time lag τ for an attractor to be in two-dimensional phase space is one fourth of the wavelength, $\gamma / 4$. In this study, the HRV signals for all participants are not typical sine waves, therefore, the goal was to reconstruct the attractor so that its maximum expansion in two-dimensional phase space was determined by computing various time delays τ experimentally to identify its maximum size in phase space. As shown in Fig. 5, the typical fixed time delay $\tau = 100$ has been used for all nine attractors reconstructed. In the next section, the statistical analysis has been shown for the cohort of individuals.

Statistical Analysis of the Complexity Matching

To further second the hypothesis of this study, the statistical analysis is performed. The statistical analysis helps to corroborate the mathematical interpretation of the complexity matching and to visualize the overall pattern of the HRV during the phases of meditation as shown in Fig. 6. It was decided to employ the boxplot representation and analyze it for the cohort of Healers and Healee over the nine consecutive phases of the experiment. In Fig. 6, the x-axis represents the evenly spaced vertical lines where the box plots are plotted in each

Table 2. The Median, Minimum and Maximum Values and the Percentile Values are Tabulated for the Boxplots for the Healers and the Healee.

	Mean μ		*Standard deviation* σ		*Upper Limit* u_A	*Lower Limit* u_B
Phases	*Healers* A	*Healees* B	*Healers* A	*Healees* B	*(75^{th} Percentile of the Healers (A))*	*(25^{th} Percentile of the Healees (B))*
1st	$\mu_{1A} = 35.82$	$\mu_{1B} = 57.18$	$\sigma_{1A} = 1.97$	$\sigma_{1B} = 11.82$	37.77	44.85
2nd	$\mu_{2A} = 37.71$	$\mu_{2B} = 61.45$	$\sigma_{2A} = 2.62$	$\sigma_{2B} = 13.26$	39.55	48.00
3rd	$\mu_{3A} = 35.12$	$\mu_{3B} = 62.44$	$\sigma_{3A} = 4.99$	$\sigma_{3B} = 12.78$	38.21	51.28
4th	$\mu_{4A} = 36.01$	$\mu_{4B} = 33.03$	$\sigma_{4A} = 2.96$	$\sigma_{4B} = 2.70$	38.54	31.00
5th	$\mu_{5A} = 38.19$	$\mu_{5B} = 46.49$	$\sigma_{5A} = 3.90$	$\sigma_{5B} = 16.45$	41.33	32.71
6th	$\mu_{6A} = 37.56$	$\mu_{6B} = 33.50$	$\sigma_{6A} = 4.14$	$\sigma_{6B} = 8.52$	39.21	27.28
7th	$\mu_{7A} = 42.75$	$\mu_{7B} = 39.11$	$\sigma_{7A} = 2.62$	$\sigma_{7B} = 7.45$	44.87	32.57
8th	$\mu_{8A} = 47.75$	$\mu_{8B} = 43.01$	$\sigma_{8A} = 3.19$	$\sigma_{8B} = 12.82$	50.26	34.42
9th	$\mu_{9A} = 42.54$	$\mu_{9B} = 40.71$	$\sigma_{9A} = 1.80$	$\sigma_{9B} = 6.11$	44.51	36.00

Table 3. Statistical Conditions Validated for the Nine Phases of the Healing Circle Meditation.

Phases	$\mu_B - \sigma_B$	$\mu_A + \sigma_A$	*Statistical condition* $(\mu_B - \sigma_B) > u_B \& (\mu_A + \sigma_A) < u_A$	*Outcome*
1st	37.79	45.36	37.79> 44.85 & 45.36< 37.77	Condition is not satisfied
2nd	40.33	48.19	40.33> 48 & 48.19<39.55	Condition is not satisfied
3rd	40.11	49.66	40.11> 51.28 & 49.66< 38.21	Condition is not satisfied
4th	38.97	30.33	38.97>38.54 & 30.33<31	Condition is not satisfied
5th	42.08	30.04	42.08>32.71 & 30.04<41.33	Condition is Satisfied
6th	41.70	24.98	41.70>27.28 & 24.98<39.21	Condition is Satisfied
7th	45.36	31.66	45.36>32.57&31.66<44.87	Condition is Satisfied
8th	50.94	30.20	50.94>34.42 & 30.20<50.26	Condition is Satisfied
9th	44.34	34.60	44.34>36 & 34.60<44.51	Condition is Satisfied

phase. It should be noted that the boxplots are displayed according to the phases indicated in Table 1, but for better visualization, the boxplots in Fig. 6 are positioned in equal spaced places along the x-axis. In Fig. 6, the y-axis indicates the scale from 0 to 100. The statistical characteristics of the boxplot that are assessed are the mean (μ), standard deviation (σ), 25th percentile, 75th percentile as shown in Tables 2 and 3. The black boxplots represent the averaged H-rank of all Healers, whereas the red boxplots represent the H-rank of the Healee. First the two hypotheses are defined: Hypothesis One: "The means of the averaged H-rank of the Healers and the Healee are equal". Hypothesis Two: "The means of the averaged H-rank of the Healers and the Healee are not equal."

To validate the suggested hypothesis, a decision support statistical condition is also proposed. To begin with, first the mean and standard deviation of the averaged Healers H-rank and Healee H-rank are computed. Then with the implication of one sigma rule, the upper $\mu_A + \sigma_A$ and lower $\mu_A - \sigma_A$ boundaries are defined (see Tables 2 and 3). The statistical condition is formulated as: $(\mu_B - \sigma_B) > u_B$ & $(\mu_A + \sigma_A) < u_A$; where u_A is the 75th percentile of the Healers and the u_B is the 25th percentile of the Healee. The percentiles will be used as a variation interval to analyze the conditions in each phase of the experiment. In other words, the variation intervals u_A and u_B will serve as a baseline for assessing whether one of the two hypotheses should be accepted or rejected. For instance, if the condition $(\mu_B - \sigma_B) > u_B$ and $(\mu_A + \sigma_A) < u_A$ holds true, it signifies that it must be inside the variation interval, and the hypothesis one is eventually accepted. If the conditions are not satisfied, hypothesis one is rejected, and the second hypothesis is ultimately accepted. The statistical analysis outcomes are discussed in the sections that follow.

Comparison of the Efficacy of the H-rank Approach vs the Permutation Entropy

The efficacy of the H-rank technique is assessed by comparing it to Permutation Entropy (PE) technique. PE is a robust time series analysis tool which provides a quantification measure of the complexity of a time series by capturing the order relations between values of this time series. PE has been introduced by (Bandt & Pompe, 2002), and is extensively used for the quantification of complexity of different technological (Landauskas et al., 2020), financial (Li, Shang, & Zhang, 2019), biological processes (Mansourian, Sarafan, Torkamani-Azar, Ghirmai, & Cao, 2023). We are employing the efficient validated PE algorithm (Unakafova & Keller, 2013) for the computation of complexity matching between the Healers and the Healee. The idea of comparison between the H-rank technique and the PE is simple and straightforward. It is aimed to investigate if the PE technique will reveal the complexity matching of HRV between the group of Healers and the Healee during the meditation protocol for the nine phases of the experiment.

RESULTS

During the healing protocol, the heart rate variability data of the nine

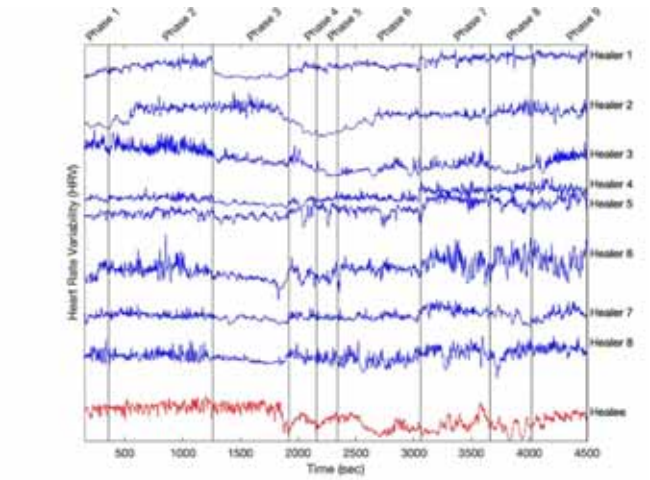

Fig. 2. HRV is monitored and registered for eight Healers and one Healee, shown here as the IBI. The blue plots depict the time series of HRV for Healers (RR-cardiac interval). The Healer's HRV is depicted in red. The experiment is windowed such that the Healee's as well as the eight Healers' HRV signal can be observed and analyzed from the beginning to the end of the experiment.

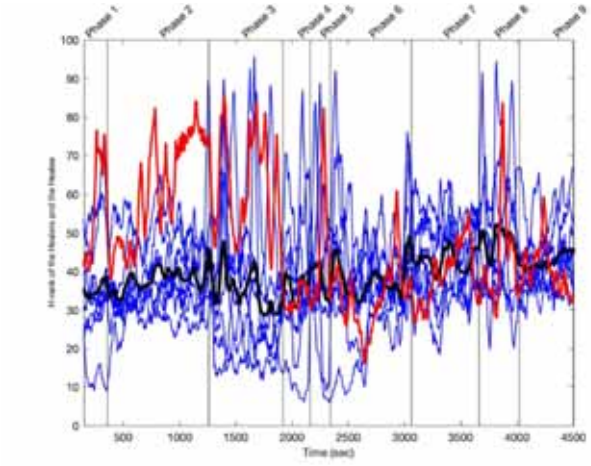

Fig. 3. The H-ranks graph for the participants is constructed throughout the experiment. (a) The blue plot depicts the H-ranks for eight Healers. (b) The arithmetic mean of the H-ranks for eight Healers is plotted in black. (c) The red plot shows the Healee's H-ranks. The x-axis represents time in seconds, while the y-axis represents the algebraic complexity of the RR- cardiac interval manipulated using H- ranks.

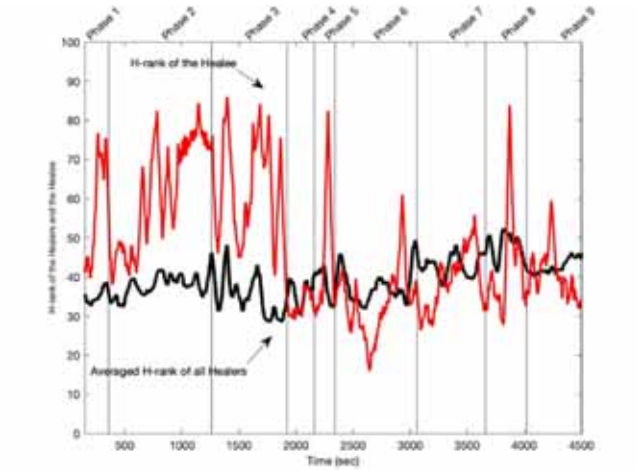

Fig. 4. The H-ranks graph for both participants is constructed throughout the experiment. (a) The arithmetic mean of the H-ranks for eight Healers is plotted in black. (c) The red plot shows the Healee's H-ranks. The x-axis represents time in seconds, while the y-axis represents the algebraic complexity of the RR- cardiac interval manipulated using H- ranks.

participants (eight Healers and one Healee) were recorded as time series. The experimental session lasted for 75 minutes which corresponds to 4500 seconds as shown in Fig. 2. In order to leverage the mathematical model for defining the algebraic complexity of the time series, the H-rank was incorporated with the range of the matrix as 150-by-150, which corresponds to the 300 consecutive data points and makes up the phase for our experiment as shown in Fig. 2. The proper selection of $\varepsilon = 0.05$ guarantees a good sensitivity of the H-rank algorithm. In Fig. 3, the Healers' H-rank has been displayed in blue graphs, the averaged H-rank for Healers is shown in black, and the Healee's H-rank is displayed in red. For the better visualization purpose, the averaged H-rank for Healers, and the Healee's H-rank is shown in Fig. 4. The x-axis is windowed for the nine phases in line with the time (in minutes) indicated in Table 1, but in the following Figs. 2, 3 and 4, the time is presented at a second's resolution.

Beginning form the very-left side of Fig. 3, is the first phase of the experiment, which corresponds to the first 6 minutes of the exercise, during which all Healers are standing outside the room where the protocol will take place. The healing protocol has not started at this point. Fig. 3 depicts that the H-rank reconstructed for Healers and Healee's appeared to have distinct trends. The averaged H-rank plots of the Healers and the Healee's H-rank plots clearly demonstrate a different mean level, which signifies the difference in the complexities of the recorder HRV signals. This suggests the lack of complexity matching.

The next activity, which lasted fifteen minutes until the 21st minute of

the exercise, is represented by the second phase. During this time period, all the Healers are now standing in the large conference room where the healing protocol will take place, and a pre-recorded guided meditation is streaming on the audio system. The Healers are advised to remain standing, close their eyes, and begin shifting their energy state as this audio begins. The differing mean level of the H-rank traces in Fig. 3 continue to suggest a lack of matching.

The third phase lasts eleven minutes until the exercise's 32nd minute. During this time, the Healers open their eyes and begin walking in a huge circle around the room, listening to guided meditation during the activity. During this time period, the closeness in matching between the reconstructed H-rank of the Healers and the Healee is not yet very observable.

The fourth phase corresponds to the HRVs observed for the following three minutes, until the exercise ends at 36 minutes. This phase corresponds to the activity when the Healers close their eyes and stand. During this time the Healees are gathering outside the conference room, waiting to enter the room, so both Healees and Healers are standing still and anticipating the healing is about to begin. During this phase we observe the matching of the reconstructed H-ranks for both the Healee and the group of Healers, with their H-ranks nearly coinciding.

The fifth phase lasted 3 minutes and corresponds to the activity in which the Healers open their eyes briefly and form healing circles (groups of 8 people sitting in a circle). Fig. 3 shows that the reconstructed H-ranks throughout this time period converge less.

The sixth phase had a duration of 12 minutes. During this time, the Healees enter the room and are instructed to lie down in the center of the healing circles of eight Healers. Healers continue standing with their eyes closed throughout this time. The H-rank constructed for this time period showed matching in the means level of their graphs during this activity period.

The seventh phase lasted for 10 minutes. The Healers are instructed to open their eyes, sit down, look at their Healee and other Healer’s briefly, before closing their eyes to begin practice changing their state to by harnessing heart-energy. The complexity matching between the reconstructed H-ranks seems to be very close for both Healers and the Healees as seen in Fig. 3.

The following phase is 6 minutes long. During this time, the Healers rub their hands together, aiming their hands towards the Healee, and begin to create a cohesive field of heart-focused energy around the Healee. Complexity matching of the reconstructed H-rank could be seen this time interval.

In the final phase, all Healers place their own hands over their hearts, and are guided to meditate on directing their heart energy inward for 8 minutes, which concludes the healing meditation protocol at 75 minutes. During this period, the apparent complexity matching continues, as perhaps the Healee is absorbing the positive energy or information transfer that appears to have occurred during the meditation phase. Statistical analysis description in the subsequent paragraph also confirms the means coming closer to each other for the averaged H-rank of the Healers and the Healee.

The trajectories’ state space realization had been explored using the

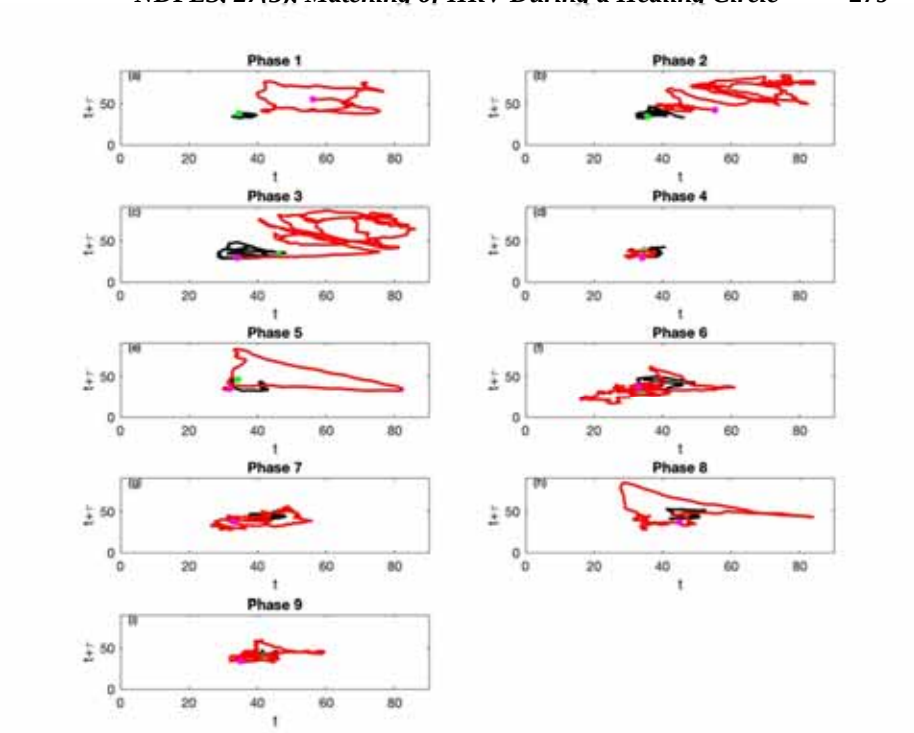

Fig. 5. The reconstruction of the embedded attractors for the group of Healers and Healee, as well as the set forth of phase plane representation. The nine trajectories have been reconstructed for the nine phases of experiment for 4500 seconds (75 min). The red trajectories are for the Healee and their beginning is marked with a magenta-filled circle, whereas the black trajectory is for the Healers and the beginning of the trajectory is marked with green-filled circle.

mathematical approaches described in detail in previous sections. Embedded attractor techniques, which are based on a direct evaluation of the geometric area occupied by the set of points of the trajectory matrix in state space with a finite range of time lag values $\tau = 100$ are implemented in this paper. Each trajectory is a representation of the complex algebraic relationship between the Healers and the Healee's H-rank, as mentioned in the preceding paragraph. The nine trajectories plotted for each of the nine phases and are shown in Fig. 5. In Fig. 5, the red trajectory represents the Healee's H-rank data points dispersed in the state space, while the black trajectory represents the average of all Healers' H-ranks. The green circle represents the start of the trajectory for the Healers, while the magenta circle represents the beginning of the H-rank trajectory for the Healee. It is worth noticing that the trajectories plotted for both the Healee and the group of Healers are relatively widely apart in the state space during the first phase. In the second time frame, the red trajectory appears to be slowly approaching the

Healer's trajectory. The third phase demonstrates that the trajectories are growing closer as the Healers open their eyes and start walking in a large circle around the room. From the fourth to the ninth trajectory, the Healee's trajectories grew progressively closer to the Healers' trajectories providing strong computational evidence of increased complexity matching during the later phases of the healing process.

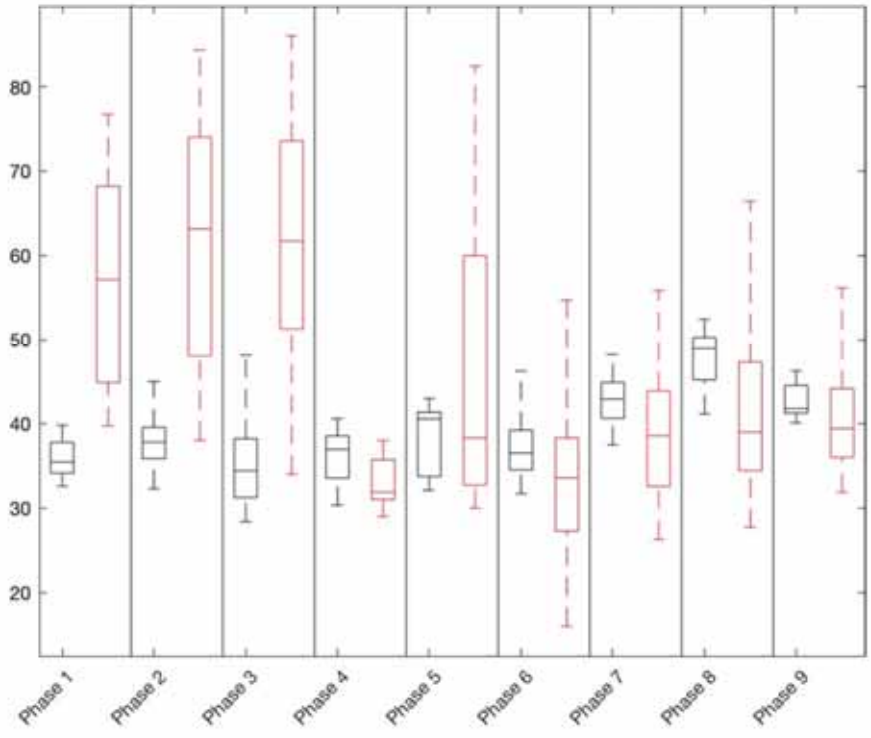

Fig. 6. Statistical analysis of the H-rank for the cohort of Healers and the Healee. The boxplots have been represented for the nine phases of the experiment. The x-axis shows the time intervals (equally spaced). The y-axis is classified from 0-100 scaling. We can see the median, 25th quartile, 75th quartile and the minimum and maximum values of each boxplot (see Table 2 & Table 3). The black boxplot shows the averaged H-rank of all the Healers throughout the meditation exercise. The red boxplot shows the H-rank of the Healee's HRV during the meditation exercise.

The statistical analysis of the averaged H-rank of the Healers and Healer allowed us to confirm our hypothesis of complexity matching of the reconstructed H-rank as well as assess the dynamical transitions from one phase to another during the healing protocol. The statistical results show that for the initial four phases of the experiment, the statistical condition $(\mu_B - \sigma_B) > u_B$ & $(\mu_A + \sigma_A) < u_A$

does not hold true which implies that the means of the averaged H-rank of the Healers and the Healee is not equal and eventually this results in the rejection of hypothesis one. This is also depicted by the boxplot representation for the initial four phases of exercise (see Fig. 6). Upon the further analysis of the statistical outcomes for the other phases of the exercise, it is noticed that the statistical condition holds true; meaning that the means of the averaged H-rank of the Healers and the Healee lies with the variation interval, and it can also be verified in Fig. 6.

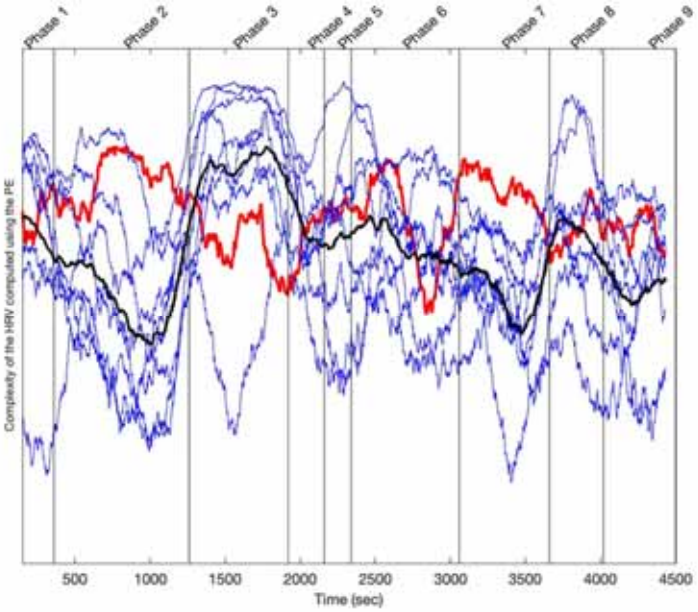

Fig. 7. Complexity of the HRV is computed using the Permutation Entropy (PE). (a) The blue lines depict the PE for each individual Healer. (b) The arithmetic mean of the PE for the eight Healers is plotted in black. (c) The red plot shows the HRV complexity measure of the Healee' by the PE method. The x-axis represents time in seconds, while the y-axis represents the complexity of the HRV computed using the PE algorithm.

The efficacy of the H-rank approach is further demonstrated by comparing it to another validated and state-of-the-art algorithm, namely Permutation Entropy (PE). The PE is used to compute the complexity matching of the HRV for both Healers and the Healee'. In Fig. 7, the x-axis shows the time in seconds, whereas the y-axis represents HRV complexity computed using the PE technique. The blue graph in Fig. 7 indicates the HRV complexity determined for each of the individual Healers, whereas the black graph represents the averaged HRV complexity computed for all the Healers. The Healee's HRV complexity is computed in red. The HRV complexity computed using the PE

approach during each phase of the exercise can be vividly seen and analyzed in the Fig. 7. It can be observed that the HRV complexity computed for both the Healers and the Healee does not seem to match at any phase of the protocol. This is strong evidence that the H-rank technique revealed the complexity matching during the phases of the meditation exercise, whereas the PE approach did not detect these important details.

The notion of incorporating and deploying the H-rank technique to reconstruct the mathematical model for defining the algebraic complexity of the HRV during the healing protocol, as well as the reconstruction of the embedded attractors technique for the state space realization of the trajectories spread in a 2-D plane, provides a clear picture of complexity matching. The convergence of the reconstructed H-rank over the course of the experiment and visualization of the increased closeness between the HRVs over the later phases of the healing process, are accomplished for the real time complex time series, which is the essence of this work. While the study's findings provide a convincing mathematical structure in the form of the H-rank approach to analyze and visualize the complexity matching that occurs between the groups during the meditation. In the end, the efficiency of the H-rank algorithm is also shown by comparing it with the PE approach.

DISCUSSION

This experiment revealed complex findings and further research will be required to better understand the many complex and subtle factors hinted at in the results. The fact that the Healers' and the Healee's HRV began portraying similar patterns during the phases of the protocol in which heart-focused healing intentions were being sent to the Healee which confirms the complexity matching that occurs in interpersonal communication and reflects the interaction effects (Joffė-Luinienė, Vainoras, & Šmigelskas, 2019). This phenomenon, however, raises additional questions about the factors that mediate such effects to occur. For instance, this study cannot establish the processes involved in modulating the closeness of the Healers and Healees reconstructed H-ranks during the healing process. For example, as shown by the attractor figures, the HRV of the Healers and the Healee becomes closer during the phases of the meditation. The question here is what mechanism generated this closeness; is it happening because of interaction (coming into the same place for both Healers and Healees)? Another question to consider is what happens if the meditation exercise is both guided and controlled. Will the result be the same or different?

These and similar questions emerging in the mind can be said to serve as definite targets for future research and are beyond the scope of the current study. As previously stated, this study demonstrates and mathematically confirms the fact that complexity matching happens for a group of individuals during a heart-coherence healing exercise.

Based on the reviewed scientific sources on physiological synchronization and their benefits (Benson et al., 2006; Tatsumura, Maskarinec, Shumay, Kakai, 2003) it can be conditionally presumed that one of the important factors in

this context is a heart-coherence state, and intention. In our experiment, Healers were lead in a heart-coherence induction activity after which focusing on transmitting positive healing intentions towards the Healee, which may be one of the key factors involved in close non-contact healing effects. Having in mind that meditation has already proved to provoke and stimulate significant transformations (McCraty et al., 2009) perhaps it makes us better able to accept that similar transformations are possible in non-contact healing processes. When we already know that such intangible feelings and emotional states as experiencing gratitude (Kyeong, Kim, Kim, Kim, & Kim, 2017) praying for yourself or others (Benson et al., 2006; Jana, 2011) etc. have objectively measurable physiological and emotional changes, then in this light our findings about the effects of distant healing are in line and contributing to the dynamic and complex perception of human health and well-being. Nonetheless, the study's goal is entirely focused on highlighting the H-rank technique as an efficient mathematical model for analyzing complexity matching and evaluating groups HRVs as a result of meditation. This research study may pave the way for future research on healing methods by providing a validated mathematical approach for assessing HRV which could be employed in a variety of experiments.

CONCLUSION

The findings of this study revealed mathematical evidence of complex interactions happening during a close non-contact healing protocol. The H-rank approach was utilized as an effective mathematical technique to illustrate the complex algebraic relationship and complexity matching between Healers and the Healee's heart rate variability. In addition to the H-rank technique, the embedding attractor approach was used to visualize the complexity matching during the various phases of a healing protocol.

The Hankel matrix technique proved to be an effective mathematical approach for defining the algebraic complexity of the reconstructed H-ranks during the healing protocol, and the reconstruction of an embedded attractors technique for the state space realization of the trajectories spread in a 2-D plane, provided a clear picture of the reconstructed H-rank becoming closer. These results could be used to encourage and stimulate the subsequent scientific studies of comparable circumstances when studying complexity matching.

Perceiving the subtle, emotional processes involved in human interactions can often be challenging, however, these findings undoubtedly show that relationships are complex, dynamic, and have great potential for better understanding the coordinated activity that occurs in various contexts involving human interactions.

ACKNOWLEDGMENTS

The author(s) received no financial support for the research, authorship, and/or publication of this article.

REFERENCES

Abney, D. H., Paxton, A., Dale, R., & Kello, C. T. (2014). Complexity matching in dyadic conversation. *Journal of Experimental Psychology: General, 143*, 2304-2015.

Afonso, R. F., Kraft, I., Aratanha, M. A., & Kozasa, E. H. (2020). Neural correlates of meditation: a review of structural and functional MRI studies. *Frontiers in Bioscience-Scholar, 12*, 92-115.

Ahmadlou, M., & Adeli, H. (2012). Visibility graph similarity: A new measure of generalized synchronization in coupled dynamic systems. *Physica D: Nonlinear Phenomena, 241*, 326-332.

Astolfi, L., Toppi, J., De Vico Fallani, F., Vecchiato, G., Salinari, S., Mattia, D., … & Babiloni, F. (2010). Neuroelectrical hyperscanning measures simultaneous brain activity in humans. *Brain Topography, 23*, 243-256.

Bandt, C., & Pompe, B. (2002). Permutation entropy: A natural complexity measure for time series. *Physical Review Letters, 88*(17), 174102. doi: 10.1103/PhysRevLett.88.174102

Behan, C. (2020). The benefits of meditation and mindfulness practices during times of crisis such as COVID-19. *Irish journal of psychological medicine, 37*, 256-258.

Benson, H., Dusek, J. A., Sherwood, J. B., Lam, P., Bethea, C. F., Carpenter, W., Levitsky, S., Hill, P. C., Clem Jr, D. W., & Jain, M. K. (2006). Study of the Therapeutic Effects of Intercessory Prayer (STEP) in cardiac bypass patients: A multicenter randomized trial of uncertainty and certainty of receiving intercessory prayer. *American Heart Journal, 151*, 934-942.

Bilek, E., Ruf, M., Schäfer, A., Akdeniz, C., Calhoun, V. D., Schmahl, C., … Meyer-Lindenberg, A. (2015). Information flow between interacting human brains: Identification, validation, and relationship to social expertise. *Proceedings of the National Academy of Sciences, 112*, 5207-5212.

Brown, R., Rulkov, N. F., & Tracy, E. R. (1994). Modeling and synchronizing chaotic systems from time-series data. *Physical Review E, 49*, 3784.

Cleeland, C. S., Gonin, R., Hatfield, A. K., Edmonson, J. H., Blum, R. H., Stewart, J. A., & Pandya, K. J. (1994). Pain and its treatment in outpatients with metastatic cancer. *New England Journal of Medicine, 330*, 592-596.

Clermont, G., & Angus, D. (2001). Towards understanding pathophysiology in critical care: the human body as a complex system. In *Yearbook of Intensive Care and Emergency Medicine 2001* (pp. 13-22). Springer.

Cohen, S., Janicki-Deverts, D., Turner, R. B., & Doyle, W. J. (2015). Does hugging provide stress-buffering social support? A study of susceptibility to upper respiratory infection and illness. *Psychological Science, 26*, 135-147.

Davidson, R. J., Kabat-Zinn, J., Schumacher, J., Rosenkranz, M., Muller, D., Santorelli, S. F., Urbanowski, F., Harrington, A., Bonus, K., & Sheridan, J. F. (2003). Alterations in brain and immune function produced by mindfulness meditation. *Psychosomatic Medicine, 65*, 564-570.

de Godoy, M. F. (2016). Nonlinear analysis of heart rate variability: a comprehensive review. *Journal of Cardiology and Therapy, 3*, 528-533.

De Vico Fallani, F., Nicosia, V., Sinatra, R., Astolfi, L., Cincotti, F., Mattia, D., … He, B. (2010). Defecting or not defecting: how to "read" human behavior during cooperative games by EEG measurements. *PloS One, 5*(12), e14187. doi:10.1371/journal.pone.0014187

Delice, F., Rousseau, M., & Feitosa, J. (2019). Advancing teams research: What, when, and how to measure team dynamics over time. *Frontiers in Psychology, 10*, 1324.

Ellingsen, D.-M., Isenburg, K., Jung, C., Lee, J., Gerber, J., Mawla, I., Sclocco, R., Jensen,

K. B., Edwards, R. R., & Kelley, J. M. (2020). Dynamic brain-to-brain concordance and behavioral mirroring as a mechanism of the patient-clinician interaction. *Science Advances, 6*(43), eabc1304.

Fine, J. M., Likens, A. D., Amazeen, E. L., & Amazeen, P. G. (2015). Emergent complexity matching in interpersonal coordination: Local dynamics and global variability. *Journal of Experimental Psychology: Human Perception and Performance, 41*, 723-737.

Fishburn, F. A., Murty, V. P., Hlutkowsky, C. O., MacGillivray, C. E., Bemis, L. M., Murphy, M. E., … Perlman, S. B. (2018). Putting our heads together: interpersonal neural synchronization as a biological mechanism for shared intentionality. *Social Cognitive and Affective Neuroscience, 13*, 841-849.

Fusaroli, R., & Tylén, K. (2012). Carving language for social coordination: A dynamical approach. *Interaction Studies, 13*, 103-124.

González-Miranda, J. M. (2002). Amplitude envelope synchronization in coupled chaotic oscillators. *Physical Review E, 65*(3), 036232.

Gotink, R. A., Meijboom, R., Vernooij, M. W., Smits, M., & Hunink, M. M. (2016). 8-week mindfulness based stress reduction induces brain changes similar to traditional long-term meditation practice–a systematic review. *Brain and Cognition, 108*, 32-41.

Guastello, S. J., Mirabito, L., & Peressini, A. F. (2020). Autonomic synchronization under three task conditions and its impact on team performance. *Nonlinear Dynamics, Psychology, and Life Sciences, 24*, 79-104.

Guastello, S. J., & Peressini, A. F. (2017). Development of a synchronization coefficient for biosocial interactions in groups and teams. *Small Group Research, 48*, 3-33.

Hansun, S. (2013). *A new approach of moving average method in time series analysis. 2013 conference on new media studies* (CoNMedia), DOI: 10.1109/CoNMedia.2013.6708545

Hoon, Y., Mohd Radzi, M. A., Mohd Zainuri, M. A. A., & Zawawi, M. A. M. (2019). Shunt active power filter: A review on phase synchronization control techniques. *Electronics, 8*, 791. doi:10.3390/electronics8070791

Hunter, J. S. (1986). The exponentially weighted moving average. *Journal of Quality Technology, 18*, 203-210.

Jana, A. (2011). How prayer works. *Indian Journal of Psychiatry, 53*, 79. doi:10.4103/0019-5545.75549

Joffė-Luinienė, R., Vainoras, A., & Šmigelskas, K. (2019). Local geomagnetic field fluctuations relationship with mental and physical health among adults in Lithuania. *Journal of Complexity in Health Sciences, 2*, 29-33.

Kawasaki, M., Yamada, Y., Ushiku, Y., Miyauchi, E., & Yamaguchi, Y. (2013). Inter-brain synchronization during coordination of speech rhythm in human-to-human social interaction. *Scientific reports, 3*, 1-8.

Kazi, S., Khaleghzadegan, S., Dinh, J. V., Shelhamer, M. J., Sapirstein, A., Goeddel, L. A., Chime, N. O., Salas, E., & Rosen, M. A. (2021). Team physiological dynamics: A critical review. *Human Factors, 63*, 32-65.

Khalsa, D. S. (2015). Stress, meditation, and Alzheimer's disease prevention: where the evidence stands. *Journal of Alzheimer's Disease, 48*, 1-12.

Koike, T., Tanabe, H. C., Okazaki, S., Nakagawa, E., Sasaki, A. T., Shimada, K., … Bosch-Bayard, J. (2016). Neural substrates of shared attention as social memory: A hyperscanning functional magnetic resonance imaging study. *NeuroImage, 125*, 401-412.

Kyeong, S., Kim, J., Kim, D. J., Kim, H. E., & Kim, J.-J. (2017). Effects of gratitude meditation on neural network functional connectivity and brain-heart coupling. *Scientific reports, 7*, 1-15.

Ladyman, J., Lambert, J., & Wiesner, K. (2013). What is a complex system? European *Journal for Philosophy of Science, 3*, 33-67.

Landauskas, M., Cao, M., & Ragulskis, M. (2020). Permutation entropy-based 2D feature extraction for bearing fault diagnosis. *Nonlinear Dynamics, 102*, 1717-1731.

Landauskas, M., Navickas, Z., Vainoras, A., & Ragulskis, M. (2017). Weighted moving averaging revisited: an algebraic approach. *Computational and Applied Mathematics, 36*, 1545-1558.

Lardone, A., Liparoti, M., Sorrentino, P., Rucco, R., Jacini, F., Polverino, A., … Sorriso, A. (2018). Mindfulness meditation is related to long-lasting changes in hippocampal functional topology during resting state: A magnetoencephalography study. *Neural Plasticity, 2018*.

Lehrer, P., Sasaki, Y., & Saito, Y. (1999). Zazen and cardiac variability. *Psychosomatic Medicine, 61*, 812-821.

Li, J., Shang, P., & Zhang, X. (2019). Financial time series analysis based on fractional and multiscale permutation entropy. *Communications in Nonlinear Science and Numerical Simulation, 78*, 104880. doi:

Light, K. C., Grewen, K. M., & Amico, J. A. (2005). More frequent partner hugs and higher oxytocin levels are linked to lower blood pressure and heart rate in premenopausal women. *Biological Psychology, 69*, 5-21.

Lindhard, T., Hermann, C., & Edwards, S. D. (2021). HeartMath coherence model throws new light on Arka Dhyana intuitive meditation. *Healthcare*, 9, 9091162. doi:10.3390/healthcare9091162

Lombardi, F., Malliani, A., Pagani, M., & Cerutti, S. (1996). Heart rate variability and its sympatho-vagal modulation. *Cardiovascular Research, 32,* 208-216. doi:10.1016/0008-6363(96)00116-2

Lucchi Basili, L., & Sacco, P. L. (2020). What makes a partner ideal, and for whom? Compatibility tests, filter tests, and the mating stability matrix. *Behavioral Sciences, 10*, 48. doi:10.3990/bs10020048

Luders, E. (2014). Exploring age-related brain degeneration in meditation practitioners. *Annals of the New York Academy of Sciences, 1307*, 82-88.

Mansourian, N., Sarafan, S., Torkamani-Azar, F., Ghirmai, T., & Cao, H. (2023). Novel QRS detection based on the adaptive improved permutation entropy. *Biomedical Signal Processing and Control, 80*, 104270. DOI

Martinmäki, K., & Rusko, H. (2008). Time-frequency analysis of heart rate variability during immediate recovery from low and high intensity exercise. *European Journal of Applied Physiology, 102*, 353-360.

McCraty, R. (2004). The energetic heart: Bioelectromagnetic communication within and between people. In P. J. Rosch and M. S. Markov (Eds.), Clinical applications of bio*electromagnetic medicine* (pp. 541-562). New York: Marcel Dekker.

McCraty, R. (2017). New frontiers in heart rate variability and social coherence research: techniques, technologies, and implications for improving group dynamics and outcomes. *Frontiers in Public Health, 5*, 267. DOI: 10.3389/fpubh.2017.00267

McCraty, R., Atkinson, M., Stolc, V., Alabdulgader, A. A., Vainoras, A., & Ragulskis, M. (2017). Synchronization of human autonomic nervous system rhythms with geomagnetic activity in human subjects. *International Journal of Environmental Research and Public Health, 14*, 770.

McCraty, R., Atkinson, M., Tiller, W. A., Rein, G., & Watkins, A. D. (1995). The effects of emotions on short-term power spectrum analysis of heart rate variability. *The American Journal of Cardiology, 76*, 1089-1093.

McCraty, R., Atkinson, M., Tomasino, D., & Bradley, R. T. (2009). The coherent heart heart-brain interactions, psychophysiological coherence, and the emergence of system-wide order. Integral Review: A Transdisciplinary & Transcultural

Journal for New Thought, Research, & Praxis, 5(2).

McCraty, R., & Shaffer, F. (2015). Heart rate variability: new perspectives on physiological mechanisms, assessment of self-regulatory capacity, and health risk. *Global Advances in Health and Medicine, 4*, 46-61.

Miles, L. K., Lumsden, J., Richardson, M. J., & Neil Macrae, C. (2011). Do birds of a feather move together? Group membership and behavioral synchrony. *Experimental Brain Research, 211*, 495-503.

Murphy, M. L., Janicki-Deverts, D., & Cohen, S. (2018). Receiving a hug is associated with the attenuation of negative mood that occurs on days with interpersonal conflict. *PloS One, 13*(10), e0203522.

Naghsh, S., Ataei, M., Yazdchi, M., & Hashemi, M. (2020). Chaos-based analysis of heart rate variability time series in obstructive sleep apnea subjects. *Journal of Medical Signals and Sensors, 10*, 53.

Newberg, A. B., Serruya, M., Wintering, N., Moss, A. S., Reibel, D., & Monti, D. A. (2014). Meditation and neurodegenerative diseases. *Annals of the New York Academy of Sciences, 1307*, 112-123.

Obrist, P. A. (2012). *Cardiovascular psychophysiology: A perspective*. Springer Science & Business Media.

Palivonaite, R., & Ragulskis, M. (2014). Short-term time series algebraic forecasting with internal smoothing. *Neurocomputing, 127*, 161-171.

Palumbo, R. V., Marraccini, M. E., Weyandt, L. L., Wilder-Smith, O., McGee, H. A., Liu, S., & Goodwin, M. S. (2017). Interpersonal autonomic physiology: A systematic review of the literature. *Personality and Social Psychology Review, 21*, 99-141.

Pérez, P., Madsen, J., Banellis, L., Türker, B., Raimondo, F., Perlbarg, V., … Naccache, L. (2021). Conscious processing of narrative stimuli synchronizes heart rate between individuals. *Cell Reports, 36*(11), 109692. doi:10.1016/ j.celrep.2021.109692

Pham, T., Lau, Z. J., Chen, S. A., & Makowski, D. (2021). Heart rate variability in psychology: A review of HRV indices and an analysis tutorial. *Sensors, 21*(12), 3998. doi:10.3390/s21123998

Pikovsky, A., Rosenblum, M., & Kurths, J. (2001). *Synchronization: A universal concept in nonlinear science*. New York: Cambridge University Press.

Ragulskis, M., Lukoseviciute, K., Navickas, Z., & Palivonaite, R. (2011). Short-term time series forecasting based on the identification of skeleton algebraic sequences. *Neurocomputing, 74*, 1735-1747.

Ragulskis, M., & Navickas, Z. (2011). The rank of a sequence as an indicator of chaos in discrete nonlinear dynamical systems. *Communications in Nonlinear Science and Numerical Simulation, 16*, 2894-2906.

Ragulskis, M., Navickas, Z., Palivonaite, R., & Landauskas, M. (2012). Algebraic approach for the exploration of the onset of chaos in discrete nonlinear dynamical systems. *Communications in Nonlinear Science and Numerical Simulation, 17*, 4304-4315.

Schippers, M. B., Roebroeck, A., Renken, R., Nanetti, L., & Keysers, C. (2010). Mapping the information flow from one brain to another during gestural communication. *Proceedings of the National Academy of Sciences, 107*, 9388-9393.

Selye, H. (1956). *The stress of life*. New York: McGraw Hill.

Sharma, H. (2015). Meditation: Process and effects. *Ayu, 36*, 233. DOI: 10.4103/0974-8520.182756

Sivakumar, B. (2017). Modern nonlinear time series methods. In Bellie Sivakumar (Ed.), *Chaos in hydrology* (pp. 111-145). New York: Springer.

Stein, P. K., Carney, R. M., Freedland, K. E., Skala, J. A., Jaffe, A. S., Kleiger, R. E., & Rottman, J. N. (2000). Severe depression is associated with markedly reduced

heart rate variability in patients with stable coronary heart disease. *Journal of Psychosomatic Research, 48*, 493-500.

Steinhoff, U., Schnabel, A., Burghoff, M., Freibier, T., Thiel, F., Koch, H., & Trahms, L. (2004). Spatial distribution of cardiac magnetic vector fields acquired from 3120 SQUID positions. *Neurology and Clinical Neurophysiology, 59*, 1-6.

Stephens, G. J., Silbert, L. J., & Hasson, U. (2010). Speaker–listener neural coupling underlies successful communication. *Proceedings of the National Academy of Sciences, 107*, 14425-14430.

Steven, V. (2010). *Heart rate variability: Linear and non-linear analysis with applications in humans physiology*. Doctaral Thesis of Faculty of Electrical Engineering Kasteelpark Arenberg. Belgium.

Strogatz, S. (2003). *Sync: The emerging science of spontaneous order*. New York: Hyperion.

Sulis, W. H. (2016). Synchronization, TIGoRS, and information flow in complex systems: Dispositional cellular automata. *Nonlinear Dynamics, Psychology, and Life Sciences, 20*, 293-317.

Sun, W., Wang, S., Wang, G., & Wu, Y. (2015). Lag synchronization via pinning control between two coupled networks. *Nonlinear Dynamics, 79*, 2659-2666.

Tamm, U. (2001). Some aspects of Hankel matrices in coding theory and combinatorics. *The Electronic Journal of Combinatorics, A1-A1*, 1595. doi:10.37236/1595

Tanabe, H. C., Kosaka, H., Saito, D. N., Koike, T., Hayashi, M. J., Izuma, K., … Munesue, T. (2012). Hard to "tune in": neural mechanisms of live face-to-face interaction with high-functioning autistic spectrum disorder. *Frontiers in Human Neuroscience, 6*, 268. doi:10.3389/fnhum.2012.00268

Tatsumura, Y., Maskarinec, G., Shumay, D. M., & Kakai, H. (2003). Religious and spiritual resources, CAM, and conventional treatment in the lives of cancer patients. *Alternative Therapies in Health & Medicine, 9*(3), 64-71.

Taylor, C. B. (2010). Depression, heart rate related variables and cardiovascular disease. *International Journal of Psychophysiology, 78*, 80-88.

Timofejeva, I., McCraty, R., Atkinson, M., Alabdulgader, A. A., Vainoras, A., Landauskas, … (2021). Global study of human heart rhythm synchronization with the earth's time varying magnetic field. *Applied Sciences, 11*, 2935. doi:10.3390/app11072935

Timofejeva, I., McCraty, R., Atkinson, M., Joffe, R., Vainoras, A., Alabdulgader, A. A., & Ragulskis, M. (2017). Identification of a group's physiological synchronization with earth's magnetic field. International *Journal of Environmental Research and Public Health, 14*, 998.

Tulen, J., Bruijn, J., De Man, K., Van Der Velden, E., Pepplinkhuizen, L., & Manin't Veld, A. (1996). Anxiety and autonomic regulation in major depressive disorder: An exploratory study. *Journal of affective disorders, 40*, 61-71.

Unakafova, V. A., & Keller, K. (2013). Efficiently measuring complexity on the basis of real-world data. *Entropy, 15*, 4392-4415.

Vacharkulksemsuk, T., & Fredrickson, B. L. (2012). Strangers in sync: Achieving embodied rapport through shared movements. *Journal of Experimental Social Psychology, 48*, 399-402.

Valdesolo, P., & DeSteno, D. (2011). Synchrony and the social tuning of compassion. *Emotion, 11*, 262. doi:10.1037/a0021302

Valencia, A. L., & Froese, T. (2020). What binds us? Inter-brain neural synchronization and its implications for theories of human consciousness. *Neuroscience of Consciousness, 2020*(1), niaa010.

Vila, J., Guerra, P., Muñoz, M. A., Vico, C., Viedma-del Jesús, M. I., Delgado, L. C., … Rodríguez, S. (2007). Cardiac defense: From attention to action. *International*

Journal of Psychophysiology, 66, 169-182.

Voss, A., Schulz, S., Schroeder, R., Baumert, M., & Caminal, P. (2009). Methods derived from nonlinear dynamics for analysing heart rate variability. *Philosophical Transactions of the Royal Society A: Mathematical, Physical and Engineering Sciences, 367*, 277-296.

Wang, P., Wen, G., Yu, X., Yu, W., & Huang, T. (2018). Synchronization of multi-layer networks: From node-to-node synchronization to complete synchronization. *IEEE Transactions on Circuits and Systems I: Regular Papers, 66*, 1141-1152.

Yoon, H., Choi, S. H., Kim, S. K., Kwon, H. B., Oh, S. M., Choi, J.-W., Lee, Y. J., Jeong, D.-U., & Park, K. S. (2019). Human heart rhythms synchronize while co-sleeping. *Frontiers in Physiology, 10*, 190. https://doi.org/10.3389/fphys.2019.00190

Zhang, Q., Wang, Z., Wang, X., Liu, L., Zhang, J., & Zhou, R. (2019). The effects of different stages of mindfulness meditation training on emotion regulation. *Frontiers in Human Neuroscience, 13*, 208. doi:10.1371/journal.pone.0174279

Zhang, Y., Meng, T., Hou, Y., Pan, Y., & Hu, Y. (2018). Interpersonal brain synchronization associated with working alliance during psychological counseling. *Psychiatry Research: Neuroimaging, 282,* 103-109.

Ziaukas, P., Alabdulgader, A., Vainoras, A., Navickas, Z., & Ragulskis, M. (2017). New approach for visualization of relationships between RR and JT intervals. *PloS one, 12*(4), e0174279.

Ziemssen, T., & Siepmann, T. (2019). The investigation of the cardiovascular and sudomotor autonomic nervous system—a review. *Frontiers in Neurology, 53*.

Zou, Y., Donner, R. V., Marwan, N., Donges, J. F., & Kurths, J. (2019). Complex network approaches to nonlinear time series analysis. *Physics Reports, 787*, 1-97.